



Ru(bpy)₃²⁺/β-cyclodextrin-Au nanoparticles/nanographene functionalized nanocomposites-based thrombin electrochemiluminescence aptasensor

Chadan Chen¹ · Guobing Wei¹ · Xuelian Yao¹ · Fusheng Liao¹ · Hong Peng¹ · Jing Zhang¹ · Nian Hong¹ · Lin Cheng¹ · Hao Fan¹

Received: 10 November 2017 / Revised: 25 January 2018 / Accepted: 1 February 2018 / Published online: 16 February 2018
© Springer-Verlag GmbH Germany, part of Springer Nature 2018

Abstract

In this study, a functionalized nanocomposite-based electrochemiluminescence (ECL) sensor for detecting thrombin was developed. First, Ru(bpy)₃²⁺/β-cyclodextrin-Au nanoparticles (β-CD-AuNPs)/nanographene (NGP) composites were used to modify the glassy carbon electrode (GCE) surface, and then aptamers (TBA1 and TBA2 with a 1:1 M ratio) were labeled with ferrocene (Fc) acting as the probes and were attached to the composite via the host–guest recognition between β-CD and Fc. In the absence of thrombin, the quenching of Fc to [Ru(bpy)₃]²⁺ was maintained, and “signal-off” ECL was observed. However, because of the specific combination of the aptamer probes and thrombin, the configuration of aptamer probes changed and escaped from the electrode surface once thrombin appears, which results in the quenching disappearance, and the ECL signal was changed from “off” to “on.” Meanwhile, the application of nanocomposites amplified the effect of “signal-on.” By this strategy, thrombin was detected with high sensitivity and with a detection limit down to 0.23 pM. Moreover, the relatively simple ECL sensor exhibited excellent reproducibility with at least 6 cycles of recovering the original signal.

Keywords Electrochemiluminescence · Nanocomposites · Host–guest recognition · “Signal-on” · Thrombin

Introduction

Thrombin is a crucial serine protease of the blood coagulation system. It plays an important role in wound healing, vascular hemostasis, inflammation, tissue adhesion, and atherosclerosis [1, 2]. In addition to these physiological effects, thrombin exhibits a moderating effect on the growth of tumor cells, for example, it promotes growth at low tumor cell concentration and inhibits growth at high tumor cell concentration and even produce apoptosis effect. Furthermore, thrombin participate in the pivotal role of the activation of the tumorigenicity of normal cells and metastasis of malignant cells [3, 4]. As

one of the indicators for measuring the abnormal coagulation function of the body, the study of highly efficient method to detect thrombin is of significance for the diagnosis of diseases.

Aptamers represent a new in vitro screening technology, i.e., SELEX, by which oligonucleotide fragments that can specifically bind to proteins, small molecules, and inorganic ions can be screened from a random single-strand oligonucleotide library. As the molecular recognition elements of aptasensor, aptamers not only bind to targets with high specificity and excellent selectivity but also can be synthesized and modified easily. In addition, they are extremely stable and non-immunogenic, a wide range of ligands, as well as easy storage compared to other recognition elements [5–7]; hence, aptasensors have been extensively developed [8–10].

ECL is the combination of electrochemistry and chemiluminescence, which integrates the advantage of luminescence and electrochemical analysis technology. ECL exhibits the advantages of ideal sensitivity, good controllability, simple instrument and operation, and good repeatability [11, 12]; hence, the ECL aptasensor, which combines ECL and sensor

✉ Lin Cheng
lincheng_2003@126.com

✉ Hao Fan
fanhao11@aliyun.com

¹ Department of Pharmacy, JiangXi University of Traditional Chinese Medicine, JiangXi 330004, China

technology, has been widely developed [13, 14]. In recent years, considerable efforts have been focused on the detection of thrombin using ECL aptasensors [15–19]. For example, a sandwich ECL aptasensor that assemble thrombin aptamer on a gold electrode surface for specific recognition with thrombin has been reported, followed by another CdS-labeled aptamer, achieving anti-interference detection [20]. Another sandwich ECL sensor based on a dual-signal amplification strategy has been reported to exhibit high detection sensitivity [21]. Although these methods can effectively amplify the signal and improve the sensitivity, the detection method requires multi-step identification, and the operation is complex. Meanwhile, nanocomposites possess some properties such as large surface area, excellent conductivity, and catalytic performance, it can improve the sensitivity of the modified sensors; thus, several of the developed ECL aptasensors exploit these advantages [19, 22–24]. A “signal-off” ECL assay for the detection of thrombin utilizing *N*-(aminobutyl)-*N*-(ethylisoluminol) (ABEI)-functionalized gold nanoparticles (ABEI-AuNPs) has been reported [25], the remaining aptamer that is not connected with thrombin exhibits ECL signals after coming in contact with ABEI-AuNPs, and the amount of thrombin increases, while the ECL signal weakens. Besides, selecting Dpa-melanin CNSs as carriers of $[\text{Ru}(\text{bpy})_3]^{2+}$ to amplify signal label was go for the construction of signal-off ECL thrombin sensor [26], and the luminescence response signal decreases as a result of the blocking effect of the target protein on the electron transport. The above signal-off ECL sensor was based on the combination of aptamer and target analyte, leading to the reduction in the luminescence signal to achieve quantitative detection. However, the method exhibits some limitations because of its decreased signal, and a large background signal is required and is easily affected by other interfering substances to produce a “false signal,” thus limiting the sensitivity of the aptasensor.

In this study, after combining the characteristics of the above sensors, a functionalized nanocomposites-based ECL aptasensor for the detection of thrombin was developed (Fig. 1). β -Cyclodextrin (β -CD) is a typical annular oligosaccharide with a cone-like hollow cylindrical cavity, with an inner hydrophobic cavity and an outer hydrophilic ring. Because of its specific cavity structure, β -CD exhibits a remarkable capacity to identify and envelop guest molecules, leading to an admirable molecular assembly system between the host and guest [27]. We modified the electrode with $\text{Ru}(\text{bpy})_3^{2+}/\beta$ -cyclodextrin–Au nanoparticles (β -CD–AuNPs)/nanographene (NGP) composites. Next, the Fc-labeled aptamer probes (TBA1 and TBA2) that can specifically recognize thrombin were anchored on the electrode surface via the host–guest recognition between β -CD and Fc. The presence of thrombin enables the change in the probe structure and the disappearance of the quenching of Fc to

$[\text{Ru}(\text{bpy})_3]^{2+}$; hence, signal-on ECL is achieved. For one unit of target, thrombin can trigger multiple ECL switches that get a high sensitivity in an ideal linear calibration range from 0.4 to 1000 pM of thrombin concentrations. In addition, the probes were directly separated from the electrode surface after the combination occurred, leading to the remarkable increase in the ECL intensity; accordingly, the sensitivity of the target is improved with a detection limit of 0.23 pM. Meanwhile, all of the reactions occurred on the surface of modified electrode, and there was no need for extra separation procedure.

Experimental

Materials

Fc-labeled aptamers TBA1 (5'-Fc-GGTTGGTGTGGGTTGG-3') and TBA2 (5'-Fc-AGTCCGTGGTAGGGCAGGTTGGGGTGA-3') for specific combination with thrombin were synthesized by Takara Co. Ltd. (Dalian, China). Thrombin, bovine serum albumin (BSA), and immunoglobulinG (IgG) were purchased from Sangon Biotechnology Co., Ltd. (Shanghai, China). The detecting solution of phosphate buffer saline (PBS, pH 7.4) containing tri-*n*-propylamine (TPA) and other reagents such as sodium borohydride (NaBH_4), dimethylsulfoxide (DMSO), chloroauric acid (HAuCl_4), acetonitrile (CH_3CN), and ethanol were commercially available and of analytical-reagent grade (Dingguo Biotechnology, Inc.). The water used in all experiments was prepared from an ultrapure water system purchased from Millipore Milli-Q (USA).

Apparatus

ECL emission measurements were implemented with a model MPI-A electrochemiluminescence analyzer (Xi'an Remax Electronic Science and Technology Co. Ltd., Xi'an, China) at room temperature (25 °C), and the autolab electrochemical workstation (Metrohm Instruments Co., Swiss) was used to record electrochemical measurements. Electrochemical experiments were carried out on a 5 mL electrochemical cell with three-electrode systems, with a glass carbon electrode (GCE, diameter of 2.0 mm) as the working electrode, a platinum wire as the counter electrode, and an Ag/AgCl as the reference electrode with a saturated KCl solution, respectively. Transmission electron microscopy (TEM) image was recorded on a JEM-2000EX transmission electron microscope (JEOL, Japan) at an accelerating voltage of 300 kV, and scanning electron microscopy (SEM) image was performed with Quanta 250 scanning electron microscopy (FEI, America). A nuclear magnetic resonance spectrometer (Bruker, 400 MHz, Swiss) was used.

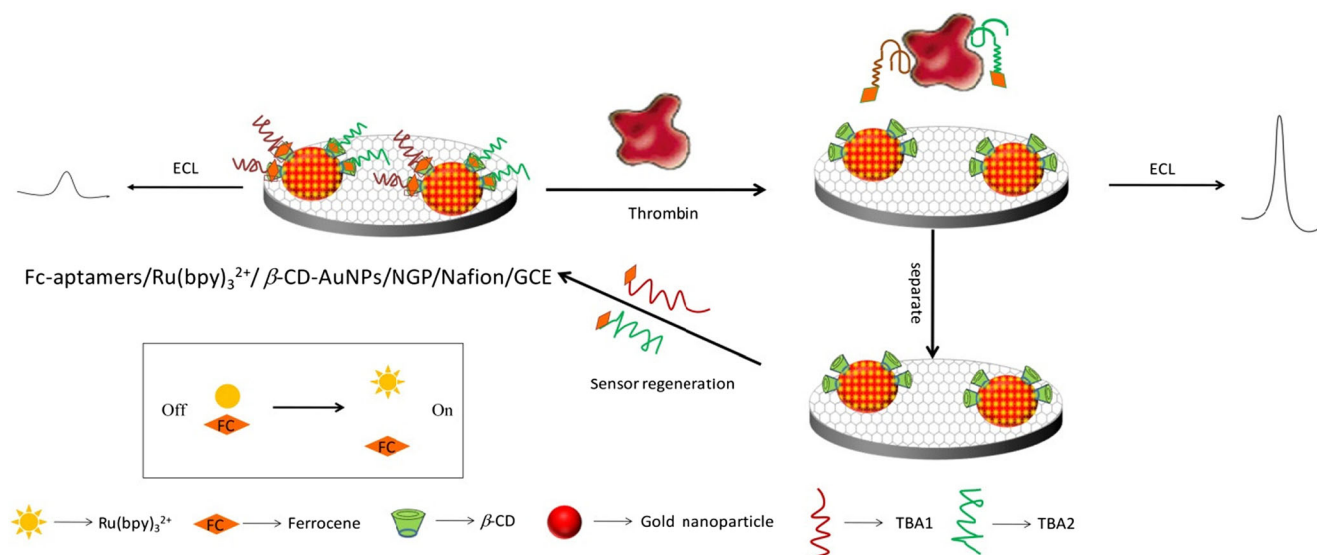


Fig. 1 Schematic of the assembly of the ECL aptasensor for the detection of thrombin

Preparation of nanographene

According to a previously reported study [28], nanographene (NGP) was prepared by ball milling. In a typical experiment, 2.0 g of graphite powder and 60 g of steel balls (diameter of 1–1.3 cm) were loaded into a hardened steel vial and purged with high-purity argon (99.999%) in a glove box for 20 min. NGP sheets were obtained by ball milling at 450 r/min for 20 h.

Preparation of β -cyclodextrin-functionalized Au nanoparticles/nanographene

Per-6-thio- β -cyclodextrin (SH- β -CD) was prepared according to a previously reported study [29] with some modifications (Supporting Information), and β -CD-AuNPs were also synthesized according to a referring literature with some modifications [30]. First, 20 mL of HAuCl_4 (0.6 mM) in aqueous DMSO ($\text{H}_2\text{O}/\text{DMSO} = 1:4$) was rapidly mixed with 16 mL of DMSO containing 8.0 mg SH- β -CD and 60.4 mg NaBH_4 , and the mixed solution was evenly stirred at room temperature for 24 h; after the addition of 32 mL of CH_3CN into the reaction mixture, the resulting precipitate was collected by centrifugation. Next, 50 mL of $\text{CH}_3\text{CN}/\text{DMSO}$ ($v/v = 1:1$) and 50 mL of ethanol were added for washing the final precipitate followed by centrifugation, and the sample was dried under vacuum at 60 °C overnight and stored for later use.

NGP (1.5 mL) and β -CD-AuNPs (0.5 mL) were mixed and stirred for 30 min, and the above process was repeated five times to make β -CD more evenly distributed over NGP. Finally, the nanocomposites (β -CD-AuNPs/NGP) were obtained and examined by TEM (Fig. 2 (left)) and SEM (Fig. 2 (right)); as can be seen from the two images, the β -CD modified AuNPs are uniformly distributed on the ordered NGP surfaces.

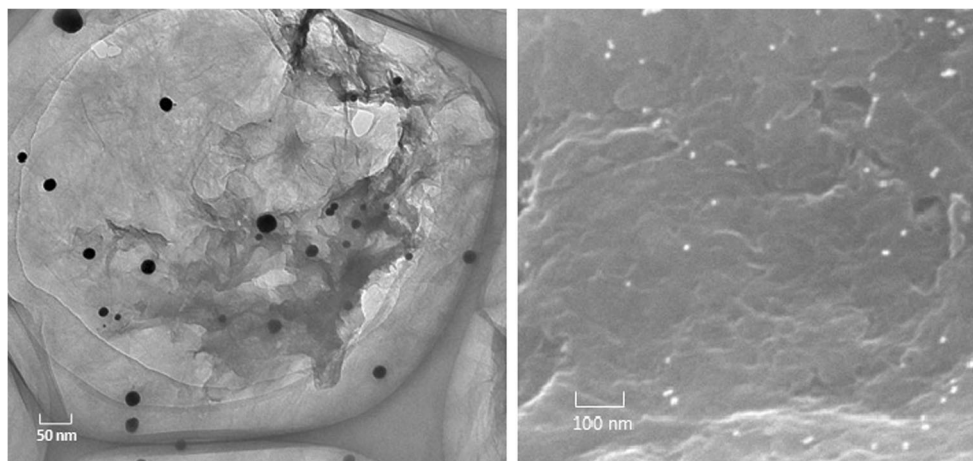
Fabrication of the ECL thrombin aptasensor

GCEs (diameter of 2 mm) were polished with 0.3- and 0.05- μm high alumina slurry and thoroughly rinsed with water. The as-obtained β -CD-AuNPs/NGP suspension was mixed with 0.5% Nafion ($v/v = 1:2$) and subjected to sonication for 30 min to afford β -CD-AuNPs/NGP/Nafion. To modify GCE with β -CD-AuNPs/NGP/Nafion, 5 μL of β -CD-AuNPs/NGP/Nafion was spin-coated on a cleaned GCE surface with a microsyringe and dried at room temperature. After dipping β -CD-AuNPs/NGP/Nafion/GCE into 1 mL of $\text{Ru}(\text{bpy})_3^{2+}$ (1 mM) for at least 30 min and thoroughly rinsing with 10 mM of phosphate buffer (PBS, pH 7.4), an ECL layer of $\text{Ru}(\text{bpy})_3^{2+}/\beta$ -CD-AuNPs/NGP/Nafion/GCE was obtained. The fabrication of the ECL thrombin aptasensor was completed with the incubation of $\text{Ru}(\text{bpy})_3^{2+}/\beta$ -CD-AuNPs/NGP/Nafion/GCE with a solution containing 0.3 mL of 0.1 mM Fc-aptamers for 60 min, and the resulting electrode surface was repeatedly eluted with 10 mM PBS (pH 7.4).

ECL sensing performance

A constant amount of thrombin was incubated with the prepared ECL thrombin aptasensor in 100 μL of 10 mM PBS (pH 7.4) for 15 min, and the excess thrombin was washed using 10 mM of PBS (pH 7.4). During this process, a three-electrode system was used to examine the ECL sensing performance. Meanwhile, a triangular potential scan at a rate of 100 mV/s in 2.0 mL of 0.1 M PBS (pH 7.4) containing 50 mM TPA was utilized for ECL measurements. The increased ECL intensity ($\Delta I = I_s - I_0$) represents the thrombin concentration, where I_0 and I_s represent the ECL intensities of the aptasensor before and after treatment with thrombin.

Fig. 2 TEM image of the prepared β -CD-AuNPs/NGP (left side). SEM image of the prepared β -CD-AuNPs/NGP (right side)



Results and discussion

Verification of the ECL intensity–potential curves for controllable electrode

Figure 3 shows the ECL intensity–potential curves using different electrodes in 0.1 M of PBS containing 50 mM TPA. As expected, no ECL signal was observed on a bare electrode (curve a in Fig. 3 (left)); however, because of the luminescent properties of $\text{Ru}(\text{bpy})_3^{2+}$ and the amplification effect of AuNPs on the $\text{Ru}(\text{bpy})_3^{2+}$, after the immobilization of $\text{Ru}(\text{bpy})_3^{2+}/\beta\text{-CD-AuNPs/Nafion}$ on the electrode, a strong ECL signal was observed (curve b in Fig. 3 (left)). With the immobilization of $\text{Ru}(\text{bpy})_3^{2+}/\beta\text{-CD-AuNPs/NGP/Nafion}$, the ECL signal changed from approximately 4900 to 8300 (curve c in Fig. 3 (left)). This change in the ECL signal is related to the excellent properties of NGP, and NGP possesses

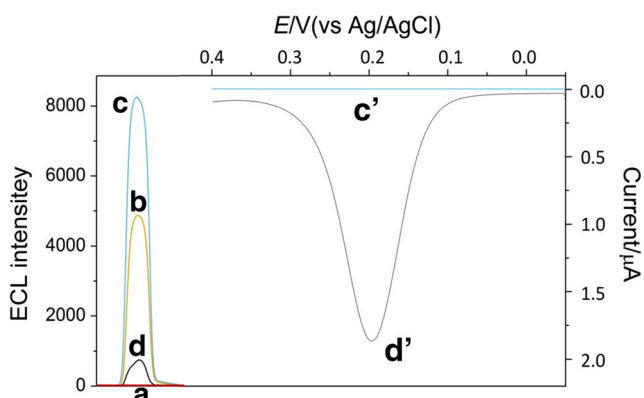


Fig. 3 ECL intensity–potential curves obtained at different electrodes in 0.1 M of PBS (pH 7.4) containing 50 mM TPA (left side). GCE (a), $\text{Ru}(\text{bpy})_3^{2+}/\beta\text{-CD-AuNPs/Nafion/GCE}$ (b), $\text{Ru}(\text{bpy})_3^{2+}/\beta\text{-CD-AuNPs/NGP/Nafion/GCE}$ (c), and Fc-aptamers/ $\text{Ru}(\text{bpy})_3^{2+}/\beta\text{-CD-AuNPs/NGP/Nafion/GCE}$ (d). The DPV responses (scanning range $-0.05\text{--}0.40\text{ V}$; scanning rate 0.002 V/s ; pulse amplitude 0.05 V) in 0.1 M of PBS (pH 7.4) for $\text{Ru}(\text{bpy})_3^{2+}/\beta\text{-CD-AuNPs/Nafion/GCE}$ (c') and Fc-aptamers/ $\text{Ru}(\text{bpy})_3^{2+}/\beta\text{-CD-AuNPs/Nafion/GCE}$ (d') (right side)

large specific surface area and subtle electron transfer; moreover, it can enhance the co-reactant diffusion in ECL-based sensors [31]. However, with the formation of a quenching monolayer of Fc on the $\text{Ru}(\text{bpy})_3^{2+}/\beta\text{-CD-AuNPs/NGP/Nafion}$ -modified electrode, the ECL of $\text{Ru}(\text{bpy})_3^{2+}$ was quenched effectively, and the ECL signal rapidly decreased (curve d in Fig. 3 (left)). The principle of ECL quenching is related to the transfer of electrons between $\text{Ru}(\text{bpy})_3^{2+}$ and ferrocenium (Fc^+), which can be verified by the suppression of radical reactions [32, 33].

Because the quenching efficiency of the ECL of $\text{Ru}(\text{bpy})_3^{2+}$ was determined by the amount of Fc-labeled aptamer probes, the differential pulse voltammetry (DPV) was used to ensure that there was sufficient Fc probes fixed to the electrode. There was almost no oxidation current with the $\text{Ru}(\text{bpy})_3^{2+}/\beta\text{-CD-AuNPs/Nafion/GCE}$ (curve c' in Fig. 3 (right)), on the contrary, a large redox current of $1.8\ \mu\text{A}$ of Fc-

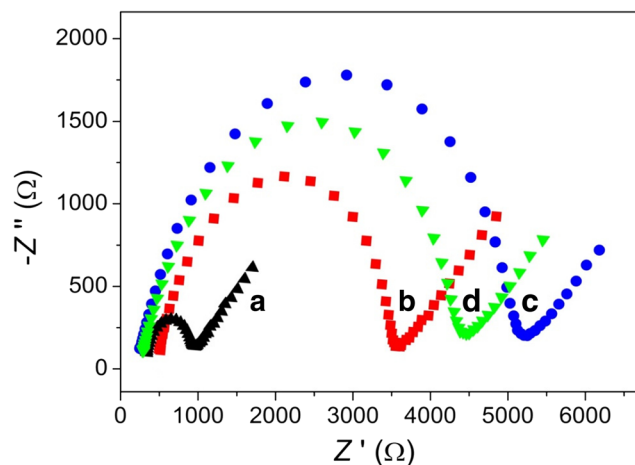


Fig. 4 Nyquist diagrams of EIS recorded from 0.1 Hz to 105 Hz for $[\text{Fe}(\text{CN})_6]^{3-}/[\text{Fe}(\text{CN})_6]^{4-}$ (10 mM, 1:1) in 0.1 M KCl. GCE (a), $\text{Ru}(\text{bpy})_3^{2+}/\beta\text{-CD-AuNPs/NGP/Nafion/GCE}$ (b), Fc-aptamers/ $\text{Ru}(\text{bpy})_3^{2+}/\beta\text{-CD-AuNPs/NGP/Nafion/GCE}$ (c), and after the incubation of Fc-aptamers/ $\text{Ru}(\text{bpy})_3^{2+}/\beta\text{-CD-AuNPs/NGP/Nafion/GCE}$ with thrombin (d)

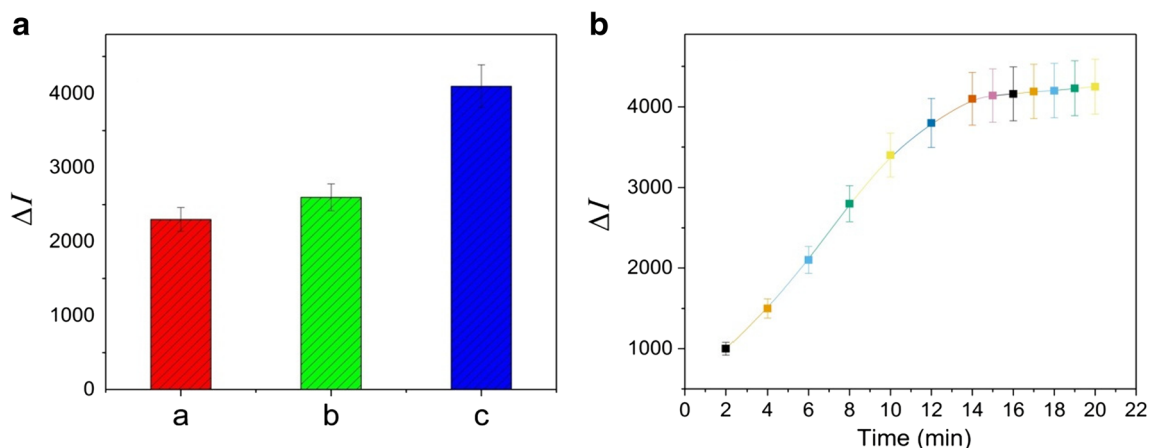


Fig. 5 **a** Response of different aptamers to the ECL aptasensor in the presence of 2 pM of thrombin, TBA1 (a), TBA2 (b), and TBA1 and TBA2 (c). **b** Effect of the incubation time of thrombin on the sensor

aptamers/Ru(bpy)₃²⁺/β-CD-AuNPs/Nafion/GCE appeared, which demonstrate the existence of a large quantity of Fc on the electrode (curve d' in Fig. 3 (right)).

Electrochemical impedance characterization of the modified electrode

Electrochemical impedance spectroscopy (EIS) was utilized to characterize the electrode assembly and detection process (Fig. 4). Bare GCE exhibited a small semicircle in the EIS spectrum (curve a in Fig. 4), indicative of the rapid electron transfer of [Fe(CN)₆⁴⁻]³⁻. Because the effective sites on the electrode surface are occupied after the immobilization of Ru(bpy)₃²⁺/β-CD-AuNPs/NGP/Nafion, the electron-transfer resistance was enhanced (Ret = 3.5 kΩ, curve b in Fig. 4). Besides, with the assembly of the aptamers on the electrode surface, the negative charges between the electrode surface and redox probe repelled each other, which limits that the rate at which the interfacial electrons are transferred and continuously increases the impedance as evidenced by Ret (from 3.5 to 5.2 kΩ, curve c in Fig. 4); in the meanwhile, this result indicated the successful assembly of the aptamers. With the

incubation of thrombin on the Fc-aptamers/Ru(bpy)₃²⁺/β-CD-AuNPs/NGP/Nafion-modified electrode, a large number of aptamers left the electrode surface, leading to significantly decreased Ret (from 5.2 to 4.5 kΩ, curve d in Fig. 4).

Selection of aptamers for sensor assembly

Because there are two sites available for the specific binding of the aptamer probes to thrombin [34], in order to achieve high sensitivity detection, TBA1 and TBA2 were selected as the detection probes to prepare the aptasensor (including 1:0 ratio; 0:1 ratio; 1:1 ratio). Figure 5a shows the response of the ECL aptasensor in the presence of 2 pM of thrombin. The sensors based on TBA1 and TBA2, respectively, exhibited relatively low responses (columns a and b in Fig. 5a). The same aptamer restricted the surface-binding sites of thrombin; thus, the ECL response with a turn-on signal to the probe decreases. However, after the immersion of both TBA1 and TBA2, the best response was obtained (column c in Fig. 5a). Based on these results, TBA1 and TBA2 (molar ratio of 1:1) were selected for constructing the ECL sensor for further experiments.

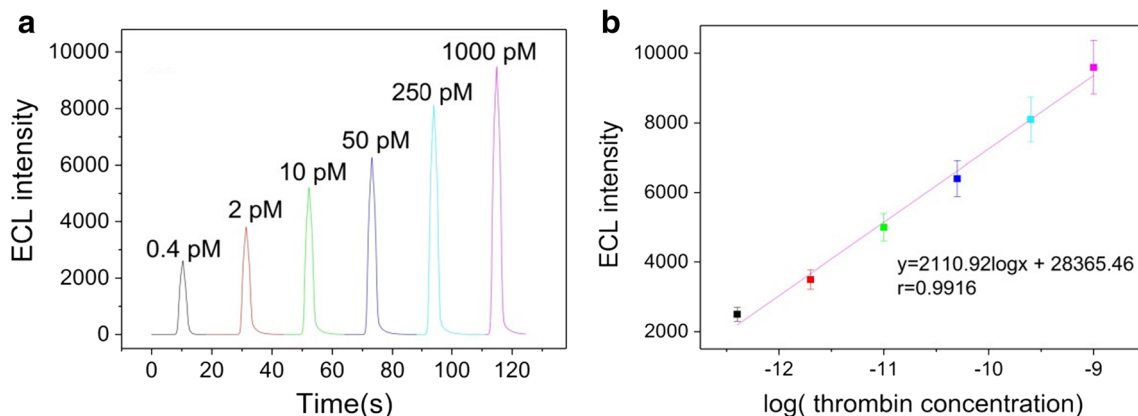


Fig. 6 **a** ECL responses to different thrombin concentrations. **b** Calibration curve of thrombin

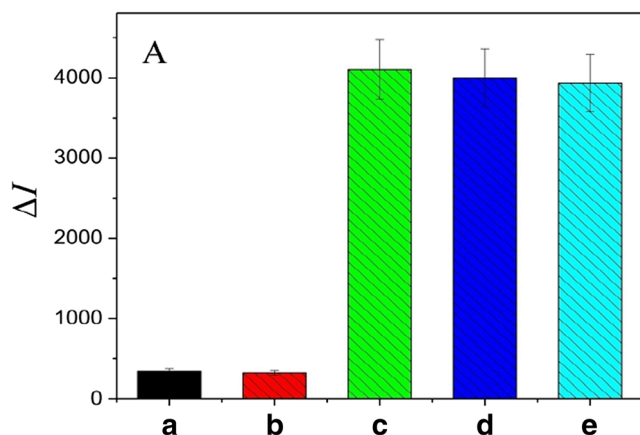


Fig. 7 Specificity of the assay for the detection of thrombin: protein concentration was maintained at 100 pM. BSA (a), IgG (b), 2 pM of thrombin (c), 2 pM of thrombin + 100 pM of BSA (d), and 2 pM of thrombin + 100 pM of IgG (e)

Optimization of the thrombin incubation time

Figure 5b shows the ECL response in terms of the incubation time on ΔI . The current signal increased with the incubation time, reaching equilibrium at 15 min. No changes were observed in ΔI after incubation for a long time, implying that the optimum incubation time for thrombin detection is 15 min. As the formation constant of the thrombin–aptamer bridge [35] is greater than that of Fc and β -CD [36], the aptamer easily binds to the binding sites of thrombin and forces Fc to leave from β -CD. Consequently, thrombin takes less time to bind to aptamers compared with the other competitive detection method [37].

Competition assay for thrombin detection

The quantitative behavior of this assay was evaluated by the variation of the thrombin concentrations under the optimized experimental conditions. With the increase of thrombin concentration, the number of Fc remaining at the electrode decreased, which leads to the enhancement of the ECL intensity (Fig. 6a). The ECL intensity was proportional to the logarithmic value of the thrombin concentration ranging from 0.4 to 1000 pM with a correlation coefficient R of 0.9916 ($n = 6$) (Fig. 6b), and the detection limit was 0.23 pM.

Table 1 Recovery results of thrombin at different concentrations spiked into human serum sample

Sample	Spiked (pM)	Found (pM)	Recovery (%)	RSD(%) $n = 3$
Serum	100.0	91.3	91.3	6.3
	200.0	183.4	91.7	4.7
	400.0	416.3	104.1	9.1
	800.0	746.5	93.3	7.8

Selectivity of the proposed aptasensor

Furthermore, the response of the aptasensor to other common interference proteins was investigated. No obvious difference was observed after the treatment with 100 pM of BSA and IgG (columns a and b in Fig. 7) compared to the blank buffer. Besides, the addition of BSA and IgG (100 pM) into the thrombin did not lead to an increase in the signal intensity (columns d and e in Fig. 7) compared to Fig. 7 column c, which further confirmed that the aptamer probes for the detection of thrombin do not interact with BSA and IgG. These results clearly demonstrated that the proposed aptasensor exhibits adequate specificity for the detection of thrombin against common interference proteins.

Actual sample analysis

To examine the practical applications of the developed aptasensor, the detection of thrombin was carried out by sample recovery experiments using 100-fold diluted healthy human serum samples, which come from volunteers of affiliated hospital of Jiangxi University of Traditional Chinese Medicine. For this purpose, different thrombin concentrations were added to the diluted healthy human serum samples, and parallel measurements were carried out in triplicate and averaged. Table 1 shows the results obtained, the sample recovery within a range from 91.3 to 104.1% with a relative standard deviation (RSD) of less than 9.1%, indicating that the ECL aptasensor efficiently detects thrombin even in complex biological environment.

Sensor regeneration

As the immobilization of the aptamer probes was achieved by the identification between the host and guest, the sensor exhibits a simple reproducibility. To examine the applicability of the prepared ECL aptasensor with Fc probes, the reusability of the sensor was examined by the anchoring of the aptamer probes (0.1 mM) on the electrode for 60 min, which could easily regenerate the sensor for further use. After treatment with thrombin, the ECL signal intensity was almost recovered to its original peak and could be recycled for at least 6 cycles (Fig. 8), which indicate the excellent reusability of the ECL aptasensor.

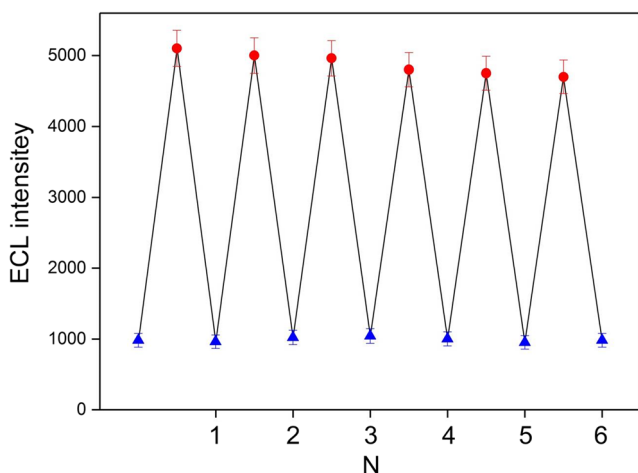


Fig. 8 Regeneration cycles of the ECL aptasensor with the stepwise challenge with 10 pM of thrombin, followed by the immersion of the Fc probes (0.1 mM) solution. N represents the times for the sensor regeneration

Conclusion

In this study, a novel thrombin ECL aptasensor was developed on the basis of host–guest recognition as well as novel nanocomposite. The new aptasensor exhibited the following characteristics: (i) high selectivity for aptamer, (ii) excellent electrical conductivity, and (iii) good ECL properties of $\text{Ru}(\text{bpy})_3^{2+}/\beta\text{-CD-AuNPs/NGP}$. As all of the reactions occurred on the GCE surface, there is no requirement for additional separation. The high specificity and sensitivity of the aptasensor are beneficial for the diagnosis of diseases caused by abnormal thrombin.

Acknowledgements This work was kindly supported by the National Natural Science Foundation of China (81660658) and (81560625), Jiangxi Science and Education Committee (GJJ160816) and (GJJ160853), Jiangxi University of Traditional Chinese Medicine Innovation Foundation (JZYC18S12).

References

- Archiniegas E, Neves CY, Candelle D, Cardier JE (2004) Thrombin and its protease-activated receptor-1 (PAR1) participate in the endothelial-mesenchymal transdifferentiation process. *DNA Cell Biol* 23(12):815–825
- Popovic M, Smiljanic K, Dobutovic B, Syrovets T, Simmet T, Isenovic ER (2012) Thrombin and vascular inflammation. *Mol Cell Biochem* 359(1–2):301–313
- Hu L, Lee M, Campbell W, Perez-Soler R, Karpatkin S (2004) Role of endogenous thrombin in tumor implantation, seeding, and spontaneous metastasis. *Blood* 104(9):2746–2751
- Nierodzik ML, Karpatkin S (2006) Thrombin induces tumor growth, metastasis, and angiogenesis: evidence for a thrombin-regulated dormant tumor phenotype. *Cancer Cell* 10(5):355–362
- Ellington AD, Szostak JW (1990) In vitro selection of RNA molecules that bind specific ligands. *Nature* 346(6287):818–822
- Kandimalla VB, Ju HX (2004) New horizons with a multi dimensional tool for applications in analytical chemistry—aptamer. *Anal Lett* 37(11):2215–2233
- Patel DJ, Suri AK (2000) Structure, recognition and discrimination in RNA aptamer complexes with cofactors, amino acids, drugs and aminoglycoside antibiotics. *J Biotechnol* 74:39–60
- Wu ZS, Zheng F, Shen GL, Yu RQ (2009) A hairpin aptamer-based electrochemical biosensing platform for the sensitive detection of proteins. *Biomaterials* 30(15):2950–2955
- Cui HF, Cheng L, Zhang J, Liu RH, Zhang C, Fan H (2014) An electrochemical DNA sensor for sequence-specific DNA recognition in a homogeneous solution. *Biosens Bioelectron* 56:124–128
- Hong N, Cheng L, Wei GB, Chen CD, He LL, Kong DL, Ceng JX, Cui HF, Fan H (2017) An electrochemical DNA. Sensor without electrode pre-modification. *Biosens Bioelectron* 91:110–114
- Zhu X, Zhang YS, Yang WQ, Liu QD, Lin ZY, Qiu B, Chen GN (2011) Highly sensitive electrochemiluminescent biosensor for adenosine based on structure-switching of aptamer. *Anal Chim Acta* 684(1–2):121–125
- Alpuche-Aviles MA, Wipf DO (2001) Impedance feedback control for scanning electrochemical microscopy. *Anal Chem* 73(20):4873–4881
- Zhang MH, Yuan R, Chai YQ, Chen SH, Zhong HA, Wang C, Cheng YF (2012) A biosensor for cholesterol based on gold nanoparticles-catalyzed luminol electrogenerated chemiluminescence. *Biosens Bioelectron* 32(1):288–292
- Wang HJ, Bai LJ, Chai YQ, Yuan R (2014) Synthesis of multi-fullerenes encapsulated palladium nanocage, and its application in electrochemiluminescence immunosensors for the detection of streptococcus suis serotype 2. *Small* 10:1857–1865
- Wang XY, Gao A, Lu CC, He XW, Yin XB (2013) An electrochemiluminescence aptasensor for thrombin using graphene oxide to immobilize the aptamer and the intercalated $\text{Ru}(\text{phen})(3)(2+)$ probe. *Biosens Bioelectron* 48:120–125
- Fang LY, Lv ZZ, Wei H, Wang EK (2008) A electrochemiluminescence aptasensor for detection of thrombin incorporating the capture aptamer labeled with gold nanoparticles immobilized onto the thio-silanized ITO electrode. *Anal Chim Acta* 628(1):80–86
- Chen Q, Chen H, Zhao YY, Zhang F, Yang F, Tang J, He PG (2014) A label-free electrochemiluminescence aptasensor for thrombin detection based on host-guest recognition between tris(bipyridine) ruthenium(II)-beta-cyclodextrin and aptamer. *Biosens Bioelectron* 54:547–552
- Zhang J, Chen PP, Wu XY, Chen JH, Xu LJ, Chen GN, Fu FF (2011) A signal-on electrochemiluminescence aptamer biosensor for the detection of ultratrace thrombin based on junction-probe. *Biosens Bioelectron* 26(5):2645–2650
- Zhuo BR, Li YQ, Huang X, Lin YJ, Chen YW, Gao WH (2015) An electrochemiluminescence aptasensing platform based on ferrocene-graphene nanosheets for simple and rapid detection of thrombin. *Sensors Actuators B Chem* 208:518–524
- Numnuam A, Chumbimuni-Torres KY, Xiang Y, Bash R, Thavarungkul P, Kanatharana P, Pretsch E, Wang J, Bakker E (2008) Aptamer-based potentiometric measurements of proteins using ion-selective microelectrodes. *Anal Chem* 80(3):707–712
- Li YJ, Li YQ, Xu N, Pan JH, Chen TF, Chen YW, Gao WH (2017) Dual-signal amplification strategy for electrochemiluminescence sandwich biosensor for detection of thrombin. *Sensors Actuators B Chem* 240:742–748
- Jie GF, Lu ZK, Zhao Y, Wang XC (2017) Quantum dots bilayers/Au@Ag-based electrochemiluminescence resonance energy transfer for detection of thrombin by autocatalytic multiple amplification strategy. *Sensors Actuators B Chem* 240:857–862

23. Liu YM, Shi GF, Zhang JJ, Zhou M, Cao JT, Huang KJ, Ren SW (2014) A novel label-free electrochemiluminescence aptasensor based on layered flowerlike molybdenum sulfide-graphene nanocomposites as matrix. *Colloid Surface B* 122:287–293
24. Wang J, Jiang XC, Han HY (2016) Turn-on near-infrared electrochemiluminescence sensing of thrombin based on resonance energy transfer between CdTe/CdS core(small)/shell(thick) quantum dots and gold nanorods. *Biosens Bioelectron* 82:26–31
25. Yu XX, Cui H (2014) Electrochemiluminescence bioassay for thrombin based on dynamic assembly of aptamer, thrombin and N-(aminobutyl)-N-(ethylisoluminol) functionalized gold nanoparticles. *Electrochim Acta* 125:156–162
26. Liu YM, Zhang JJ, Shi GF, Zhou M, Liu YY, Huang KJ, Chen YH (2014) Label-free electrochemiluminescence aptasensor using Ru(bpy)₃(2+) functionalized dopamine-melanin colloidal nanospheres and gold nanoparticles as signal-amplifying tags. *Electrochim Acta* 129:222–228
27. Bouhadiba A, Belhocine Y, Rahim M, Djilani I, Nouar L, Khatmi DE (2017) Host-guest interaction between tyrosine and (beta-cyclodextrin): molecular modeling and nuclear studies. *J Mol Liq* 233: 358–363
28. Wu LD, Deng DH, Jin J, Lu XB, Chen JP (2012) Nano-graphene-based tyrosinase biosensor for rapid detection of bisphenol A. *Biosens Bioelectron* 35(1):193–199
29. Ha W, Kang Y, Peng SL, Ding LS, Zhang S, Li BJ (2013) Vesicular gold assemblies based on host-guest inclusion and its controllable release of doxorubicin. *Nanotechnology* 24(49):495103
30. Patolsky F, Lichtenstein A, Willner I (2000) Amplified microgravimetric quartz-crystal-microbalance assay of DNA using oligonucleotide-functionalized liposomes or biotinylated liposomes. *J Am Chem Soc* 122(2):418–419
31. Chen D, Tang LH, Li JH (2010) Graphene-based materials in electrochemistry. *Chem Soc Rev* 39(8):3157–3180
32. Wang XY, Dong P, Yun W, Xu Y, He PG, Fang YZ (2010) Detection of T4 DNA ligase using a solid-state electrochemiluminescence biosensing switch based on ferrocene-labeled molecular beacon. *Talanta* 80(5):1643–1647
33. Shanguan DH, Meng L, Cao ZC, Xiao ZY, Fang XH, Li Y, Cardona D, Witek RP, Liu C, Tan WH (2008) Identification of liver cancer-specific aptamers using whole live cells. *Anal Chem* 80(3): 721–728
34. Pavlov V, Xiao Y, Shlyahovsky B, Willner I (2004) Aptamer-functionalized Au nanoparticles for the amplified optical detection of thrombin. *J Am Chem Soc* 126:11768–11769
35. Fan H, Chang Z, Xing R, Chen M, Wang QJ, He PG, Fang YZ (2008) An electrochemical aptasensor for detection of thrombin based on target protein-induced strand displacement. *Electroanalysis* 20(19):2113–2117
36. Siegel B, Breslow R (1975) Lyophobic binding of substrates by cyclodextrins in nonaqueous solvents. *J Am Chem Soc* 97(23): 6869–6870
37. Centi S, Messina G, Tombelli S, Palchetti I, Mascini M (2008) Different approaches for the detection of thrombin by an electrochemical aptamer-based assay coupled to magnetic beads. *Biosens Bioelectron* 23(11):1602–1609